J Solid State Electrochem (2007) 11:1319–1325
DOI 10.1007/s10008-007-0293-5

ORIGINAL PAPER

Electrochemical corrosion behavior of nanocrystalline zinc coatings in 3.5% NaCl solutions

Mou Cheng Li · Li Li Jiang · Wen Qi Zhang · Yu Hai Qian · Su Zhen Luo · Jia Nian Shen

Received: 15 January 2007 / Revised: 6 February 2007 / Accepted: 15 February 2007 / Published online: 8 March 2007

Abstract The corrosion behavior of electrodeposited nanocrystalline (NC) zinc coatings with an average grain size of 43 nm was investigated in 3.5% NaCl solutions in comparison with conventional polycrystalline (PC) zinc coatings by using electrochemical measurement and surface analysis techniques. Both polarization curve and electrochemical impedance spectroscopy (EIS) results indicate that NC and PC coatings are in active state at the corrosion potentials, and NC coatings have much higher corrosion resistance than PC ones. The corrosion products on both coating surfaces are mainly composed of ZnO and $Zn_5(OH)_8Cl_2{\cdot}H_2O$, but the corrosion products can form a relatively more protective layer on NC coating surfaces than on PC coatings. The EIS characteristics and corrosion processes of PC and NC zinc coatings during 330 h of immersion were discussed in detail.

Keywords Zinc · Nanocrystalline · Corrosion · EIS · Chloride

Introduction

Since nanocrystalline materials were first introduced over two decades ago [1], their corrosion properties have received extensive attention. A change in the microstructure of materials from conventional polycrystalline (PC) to nanocrystalline (NC) definitely leads to form large volume fractions of intercrystalline defects such as grain boundaries and triple junctions. The initial question is whether the great increase in these defects has a detrimental effect on corrosion performance [2].

In the literature, the corrosion behavior of a wide range of NC materials had been investigated in comparison with the PC counterparts. Some studies reported the degradation of corrosion resistance for NC materials, e.g., Ni with grain sizes of 7.5, 32, and 50 nm [3, 4] and Ni–P with grain sizes of 8.4 and 22.6 nm [5] in sulfuric acid solutions, NC $Cu_{90}Ni_{10}$ alloy in neutral chloride solutions [6], NC Co–Cu alloys in alkaline solutions [7], and surface nanocrystallized low-carbon steel in acidic sulfate solutions [8]. The increased corrosion rates of NC materials can be mainly attributed to the high volume fraction of the aforementioned defects, which provide more active corrosion sites. However, more studies observed enhanced corrosion properties with reducing grain size to nanorange (<100 nm), especially the remarkable increase in localized corrosion resistance, e.g., NC Ni [9] and milled Mg with a grain size of 34 nm [10] in alkaline solutions, NC Ti [11] and NC ingot iron [12, 13] in hydrochloric acid and sulfuric acid solutions, and NC copper [14], NC Ni–Cu alloys [15], and NC coating or surface of stainless steels [16–18] in chloride solutions. The better corrosion resistance of NC materials mainly results from their improved homogeneity and passive films or protective corrosion product layers. Obviously, these reports have demonstrated that the effect of nanostructure on corrosion behavior varies with metal systems and corrosion environments.

Zinc is a widely used material for protecting steels from corrosion, usually being used as a sacrificial coating by hot dipping or electroplating. It is of great significance to improve the properties of conventional zinc coatings

M. C. Li (✉) · L. L. Jiang · W. Q. Zhang · J. N. Shen
Institute of Materials, Shanghai University,
149 Yanchang Road,
Shanghai 200072, People's Republic of China
e-mail: mouchengli@yahoo.com.cn

Y. H. Qian · S. Z. Luo
Technology Center, Baoshan Iron and Steel,
Fujin Road,
Shanghai 201900, People's Republic of China

through nanotechnology. Several NC zinc electrodeposits were obtained from various electrolytes (e.g., acetate-based bath [19], chloride-based bath [20, 21], and sulfate-based bath [22, 23]). The corrosion behavior of NC zinc has been scarcely studied to date. One NC zinc coating with a grain size of 56 nm showed higher corrosion resistance in alkaline solution than the PC one [24].

Chloride-ion-induced corrosion is a common situation for protective zinc coatings such as in marine environments. In this work, the corrosion behavior of NC zinc coatings with grain size of 43 nm as well as the PC ones was investigated in simulated seawater by electrochemical measurement techniques. The main purposes are to get a deeper understanding of electrochemical corrosion characteristics for NC zinc and to offer fundamental information for developing new NC zinc coatings.

Experimental

Preparation of zinc coatings

The pulse electrodeposition was used to prepared zinc coatings in a two-electrode cell. A platinum foil served as the anode (about 1 cm^2). Cold-rolled low-carbon steel specimens were used as cathode with an exposed surface area of about 0.1 cm^2. Before each plating experiment, the specimen surface was ground with 800 grit waterproof abrasive paper and then pickled in 10 wt% H_2SO_4 at room temperature for 30 s. The anode and cathode were fixed with a space of about 5 cm and immersed vertically into the plating solution about 3-cm lower than the solution surface. The plating solutions were made of 350 g/l $ZnSO_4{\cdot}7H_2O$ with or without organic additives, maintained at 23±2 °C, and agitated slowly by a magnetic stirrer. The pH value was adjusted to about 1 by dilute H_2SO_4. Polyethylene glycol ($C_{2n}H_{4n+2}O_{n+1}$) with a mean molecular weight 600 g/mol, cetyltrimethylammonium bromide ($C_{19}H_{42}BrN$), benzalacetone ($C_{10}H_{10}O$), and thiourea (CH_4N_2S) were used in combination as additives. According to a previous study [23], zinc electrodeposits were prepared by applying a galvanostatic square wave for 10 min with a pulse peak current density of 2 A/cm^2. The current-on time and current-off time were set at 4 and 8 ms, respectively. PAR (Princeton Application Research, AMETEK) system, which comprised an M273A potentiostat/galvanostat, and the PowerSuite software, was used to generate the current waveforms and supply the current.

Electrochemical corrosion tests

The 3.5% NaCl solution (open to air at 25±2 °C) was used as corrosive medium. Electrochemical experiments were performed in a three-electrode glass cell. A saturated calomel electrode (SCE) and a platinum foil served as the reference electrode and counter electrode, respectively. PAR system, which included an M273A potentiostat, an M5210 lock-in amplifier, and the PowerSuite software, was used for measuring corrosion potential (E_{corr}), polarization curve, and measurements by electrochemical impedance spectroscopy (EIS). All experiments were repeated by using different specimens to confirm reproducibility of the results.

Polarization curves were determined by potentiodynamical technique with a potential scan rate of 20 mV/min after the zinc-coating specimens were immersed for 10 min. The cathodic and anodic scans were performed separately, and both scans started from E_{corr}.

Measurements by EIS were conducted discontinuously during a 14-day immersion. An alternating current signal with the frequency range from 98 kHz to 10 mHz and an amplitude of 10 mV (rms) was applied to the working electrode at E_{corr}. At the same time, values of E_{corr} were recorded. EIS spectra were interpreted using the commercial ZSimpWin 3.10 software (a nonlinear least square fitting procedure).

Characterization of zinc coatings

The surface morphology and grain size of the original zinc coatings were observed using scanning electron microscopy (SEM; JSM 6700F or FEI XL30). X-ray diffraction (XRD) analysis was conducted by using a Rigaku diffractometer (D/Max 2550 V) with Cu Kα irradiation (λ=0.15405 nm). The crystal size was also estimated by the Scherrer's equation $D=K\lambda/B\cos\theta$, where D is average crystal size, λ is the wavelength of the X-ray irradiation, K is usually taken as 0.89, B is the full width half maxima (FWHM) of diffraction peak corrected for the instrumental line broadening using silicon as a standard, and θ is the diffraction angle [25]. After the immersion tests, measurements by SEM and XRD were carried out for the corroded coating specimens.

Results

Characteristics of zinc coatings

Figures 1 and 2 give the SEM morphologies and XRD patterns for PC and NC zinc coatings electrodeposited from different sulfate baths, respectively. Both coatings have metallic brightness. PC coating comprises coarse zinc plates with a diameter less than about 5 μm and a (103) preferred orientation. NC coating consists of zinc particles with a size far less than 100 nm and a (101) random orientation. The average grain size is about 43 nm, calculated by the XRD

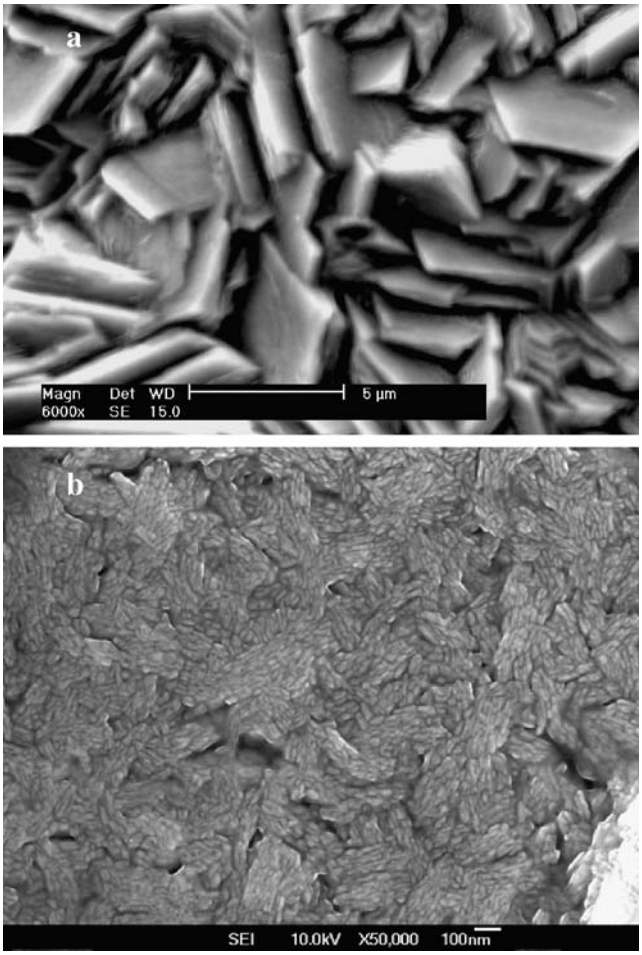

Fig. 1 SEM morphologies for **a** PC zinc coating deposited from additive-free bath and **b** NC zinc coating deposited from quarternary additive-containing bath

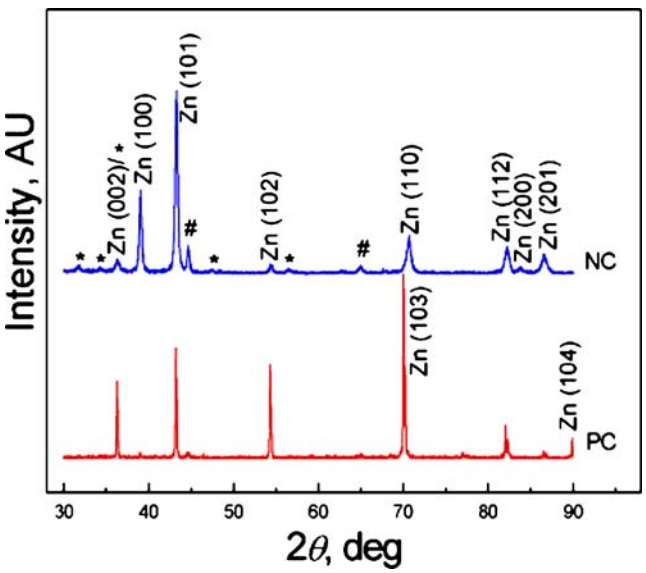

Fig. 2 XRD patterns for PC and NC zinc coatings before the corrosion tests. (*stars*, ZnO; *number sign*, steel substrate)

line-broadening value. A slight response of ZnO was identified for NC coating but was not for PC one. When zinc is exposed to the atmosphere, some oxides, such as ZnO, will be rapidly and inevitably formed on its surface [26–28]. Compared with PC zinc, NC zinc should be easier to form surface oxide because of their higher chemical activity. The response of ZnO for NC coating maybe due to the air-formed oxide on coating surface instead of a small amount of oxides in the coating as observed by Yan et al. [29].

Polarization curves

Figure 3 shows the potentiodynamic polarization curves for PC and NC zinc coatings in 3.5% NaCl solutions. Both coatings were in active state at E_{corr} and showed cathodic mass transport control in the corrosion processes. It is well known that the oxygen reduction ($O_2+2H_2O+4e\rightarrow 4OH^-$) is the major cathodic reaction of zinc corrosion in this medium. A notable difference is that the curves of NC zinc shift to the left-hand side over the entire potential range in comparison with those of PC zinc, which means that NC zinc had lower both anodic and cathodic reaction rates during corrosion process than PC zinc. Wang et al. [13] found the similar polarization behavior for bulk NC ingot iron in acidic sulfate solutions. The change indicates that the corrosion resistance of NC zinc coating is better than that of PC one.

E_{corr} vs time

To observe the relatively long-term corrosion behavior, PC and NC zinc coatings were immersed in 3.5% NaCl solutions for 330 h, respectively. During the immersion,

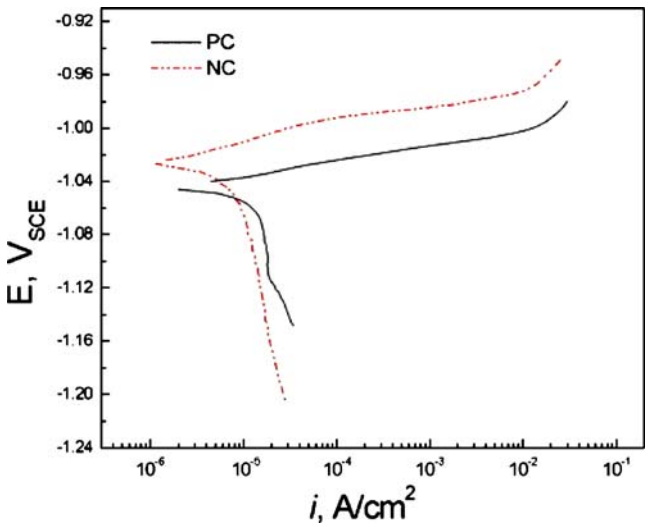

Fig. 3 Polarization curves for PC and NC zinc coatings in 3.5% NaCl solutions

E_{corr} and EIS data were determined at regular intervals. Figure 4 gives the variation of E_{corr} with exposure time for PC and NC zinc coatings in the test solutions. In both cases, the values of E_{corr} decreased soon after the coatings were immersed in the solutions and stabilized at −1.055 V_{SCE} after about 24 h of immersion. The decrease in E_{corr} was mainly related to the dissolution or evolution of the air-formed oxide thin films during the immersion [26, 27]. The stable E_{corr} indicated that the corrosion of zinc coatings attained a steady state.

EIS spectra

Figure 5 shows the typical Nyquist impedance plots for PC coating in the test solution at different times of immersion. Some curves were omitted to keep the figure clear. Experimental data were also compared with the fitted values obtained for data processing as will be described later. The curve measured at 1.5 h was composed of two depressed semicircles. Manov et al. [30] obtained a similar result of zinc in sulfate–chloride solutions. The high frequency semicircle could be attributed to the charge transfer in combination with the corrosion products. The low frequency semicircle had the appearance of diffusion process through a porous layer [31–34], i.e., finite length diffusion. The diffusion part disappeared gradually with the increase in immersion time, and eventually, the impedance curve evolved into a single capacitive semicircle. Da Silva et al. [35] observed a similar behavior of galvanized steel in chloride solutions. Whereas, the initial part in high frequencies exhibited no obvious change during 330 h of immersion as shown by the inset in Fig. 5.

EIS spectra for NC coating are given in Fig. 6. The curve at 1.5 h was similar to that of PC coating. After 48 h of immersion, the low frequency semicircle evolved as a straight line, indicating that the finite diffusion process changed to the semi-infinite diffusion. After 330 h of immersion, a new capacitive response emerged in the initial high frequency part as shown by the inset in Fig. 6. These changes were mainly ascribed to the evolution of the

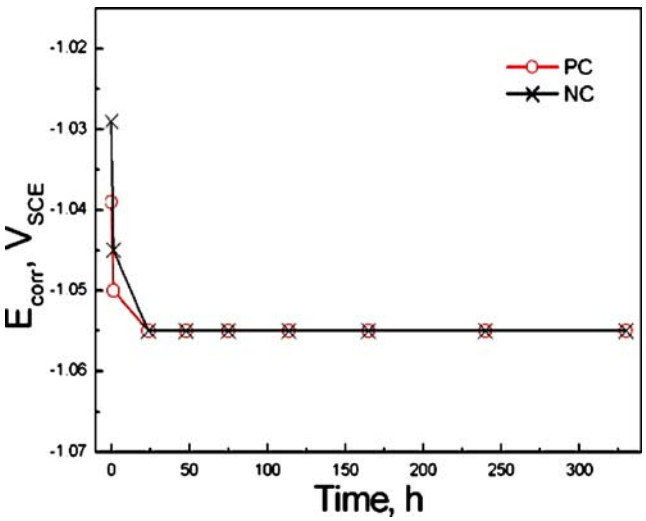

Fig. 4 Plots of E_{corr} vs time for PC and NC zinc coatings in 3.5% NaCl solutions

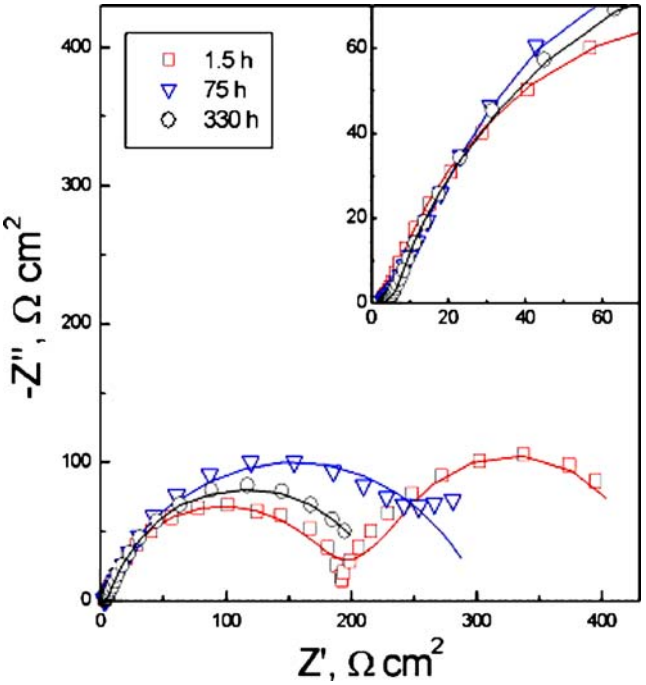

Fig. 5 Nyquist plots for PC zinc coating in 3.5% NaCl solution after different times of immersion. The *inset* shows the high frequency part. *Symbols*, experimental data; *lines*, fitted values

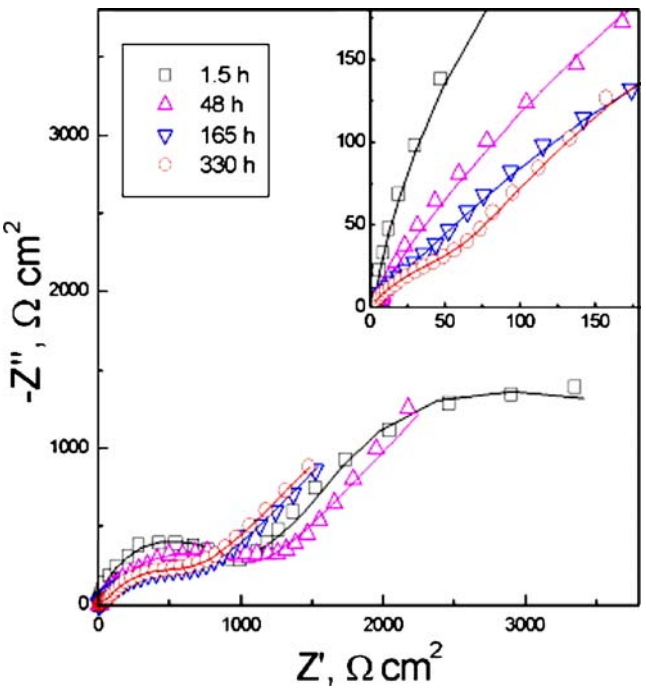

Fig. 6 Nyquist plots for NC zinc coating in 3.5% NaCl solution after different times of immersion. The *inset* shows the high frequency part. *Symbols*, experimental data; *lines*, fitted values

corrosion product layer during the immersion. Moreover, it can be seen evidently from Figs. 5 and 6 that NC coating shows much larger impedance values than PC coating.

Characteristics of corroded zinc surfaces

After 330 h of immersion, SEM observations were carried out for PC and NC coatings and are shown in Fig. 7. The images display that both surfaces are covered with corrosion product layers. For PC zinc coating, a long crack appears clearly, and a part of the corrosion products must have been detached from the coating surface during the immersion. As for NC zinc coating, some big and shallow pits distribute over the corroded surface. Many loose corrosion products exist at the bottom of the pits, as shown by the inset in Fig. 7b.

XRD analysis in Fig. 8 indicates that the corrosion product layers on both zinc-coating surfaces are mainly composed of ZnO and $Zn_5(OH)_8Cl_2{\cdot}H_2O$ (simonkolleite).

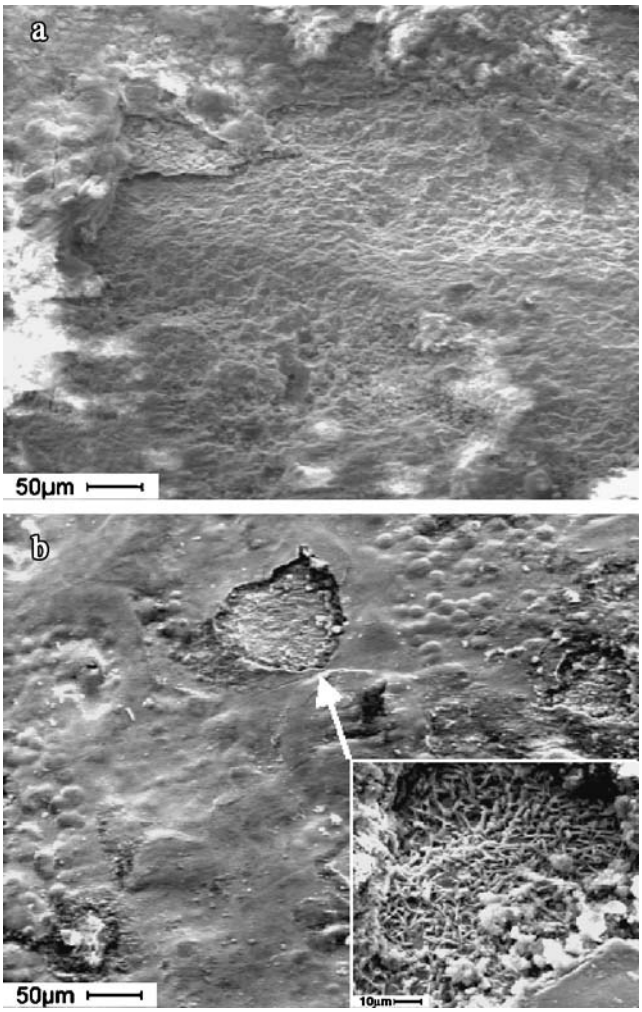

Fig. 7 SEM morphologies for corroded surfaces of **a** PC and **b** NC zinc coatings after 330 h of immersion. The *inset* shows a higher magnification image for a pit

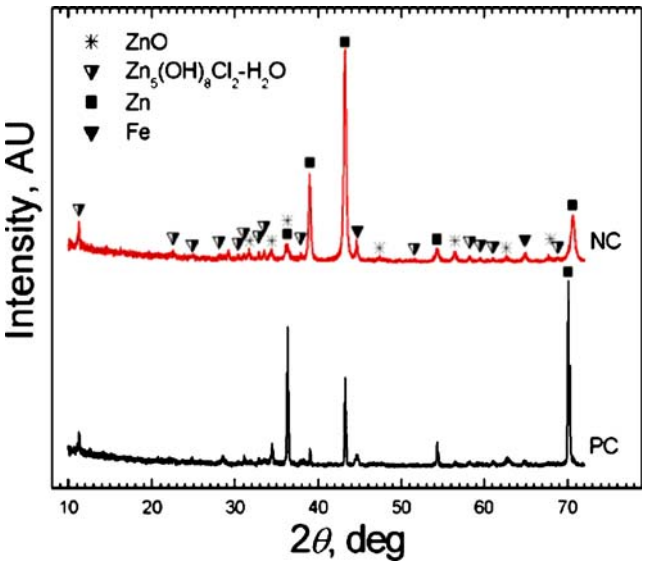

Fig. 8 XRD patterns for PC and NC zinc coatings after 330 h of immersion

These two matters are the most commonly detected corrosion products on zinc surfaces corroded in chloride-containing environments [26, 27]. There are maybe other corrosion products such as $Zn(OH)_2$, which are sometimes difficult to be found by XRD [36, 37].

Discussion

Interpretation of EIS spectra

According to the above results and the literature [30, 34, 38], a tentative equivalent circuit in Fig. 9 was proposed as a model for the corrosion system zinc/solution. R_s represents the electrolyte resistance, R_l and C_l represent the resistance and capacitance of porous corrosion product layer, and R_t and C_{dl} represent the charge transfer resistance and double layer capacitance, respectively. Z_D is a tentative element and represents three cases as follows: (1) equal to Z_O (the impedance for finite length diffusion), this case was used to fit EIS spectra obtained before 48 and 24 h for PC and NC zinc coatings, respectively; (2) equal to Z_W (the Warburg impedance for semi-infinite diffusion), this case was used to fit the spectra obtained after 48 h for NC coating; and (3) equal to a line (i.e., simply deleted). This

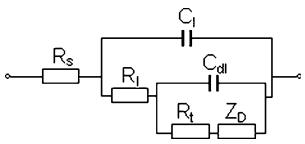

Fig. 9 A tentative equivalent circuit for the corrosion system zinc coating/solution. R_s, electrolyte resistance; R_l and C_l, resistance and capacitance of porous corrosion product layer; R_t, transfer resistance; C_{dl}, double layer capacitance; Z_D, a tentative element

case was used to fit the spectra obtained after 75 h for PC coating, although several poorly defined points may existed in the low frequency part. In addition, both C_l and C_{dl} were replaced with constant phase element (CPE) in the fitting procedure due to the non-ideal capacitive response of the interface zinc/solution.

The simulated data show good coincidence with the experimental data in spite of the approximations made, as shown in Figs. 5 and 6. It can be concluded that the above three equivalent circuit models provided a reliable description for the corrosion systems. Figure 10 gives some fitted results of EIS spectra for both coatings. The values of R_t are much larger for NC coating than for PC coating, implying that the former has higher corrosion resistance than the latter. Furthermore, both R_t reach relatively stable stages after 165 h. For a simple comparison from the ratio between the values of R_t for NC and PC coatings at 330 h, the corrosion resistance of NC coating is about 2.8 times higher than that of PC coating. One main reason is that the corrosion product layer on NC coating should be more protective than that on PC coating, as the values of R_l for NC coating are much larger. Another reason is the difference in texture between them. According to the study of Park and Szpunar [39], the (101) random orientation of NC coating should result in lower corrosion rate in comparison with the (103) preferred orientation of PC coating.

Evolution of corrosion process

Based on the above analyses, the corrosion processes of zinc coatings were simply assumed as follows. The air-formed thin films on both coatings were relatively compact so that the EIS spectra at 1.5 h (Figs. 5 and 6) were characterized by Z_O. After the zinc coatings were immersed in 3.5% NaCl solutions, the corrosion induced the dissolution of air-formed oxides or their transformation from zinc oxide to chloride corrosion products [26, 27, 38] and then the formation of microporous corrosion product layers. These changes were responsible for the drop of E_{corr}, R_l, and R_t before 24 h of immersion for both coatings (Figs. 4 and 10). Because the corrosive electrolytes could reach fresh zinc through the porous corrosion product layers, E_{corr} stabilized at about −1.055 V_{SCE} (Fig. 4) after 24 h, indicative of an active corrosion state. R_t and R_l increased after 24 h, which resulted from the evolution of corrosion product layers such as their growth and the deposition of corrosion products into the pores. With the growth of corrosion product layers, some macrodefects would form in the layers such as crack (Fig. 7a) and pit (Fig. 7b). As a result, after 165 h of immersion, the corrosion resistance (i.e., R_t) of both zinc coatings tended to decrease slightly.

Furthermore, mainly owing to the cracking or detachment of corrosion products on PC zinc-coating surface, the diffusion of oxygen disappeared with time (Fig. 5). Whereas due to the formation of a thick corrosion product layer on NC coating, although it had some macro-pits, the diffusion impedance changed form Z_O to Z_W (Fig. 6). Obviously, the existence of Z_W, especially after 330 h of immersion, was mainly attributed to the influence of corrosion products. It should be noted, of course, that zinc corrosion became complex with the evolution of the corrosion product layer. The mass transport might involve oxygen for cathodic reaction and metallic ions from the anodic process, which occurred through not only the porous corrosion product layer but also the aqueous solution [40, 41] and could be partially stimulated by chloride anions [42]. Thus, further work is necessary to elucidate the corrosion process of the zinc coatings more unambiguously.

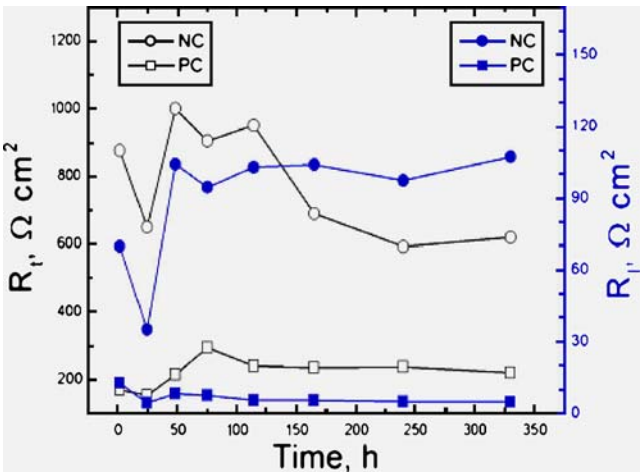

Fig. 10 Fitted results for EIS spectra of PC and NC coatings at different immersion times

Conclusion

In 3.5% NaCl solutions open to air at 25±2 °C, both NC and PC zinc coatings electrodeposited from acidic sulfate solutions are in active state at the corrosion potentials. During 330 h of immersion, NC zinc coatings show much higher corrosion resistance than the PC ones. The porous corrosion product layers can form on both coating surfaces, which seem to play an important role in the corrosion processes. In comparison with the PC zinc coatings, the enhanced corrosion resistance of NC zinc coatings is mainly due to the better protection of the corrosion product layer. ZnO and $Zn_5(OH)_8Cl_2{\cdot}H_2O$ are detected on both corroded coating surfaces by XRD, showing no significant difference between the corrosion products of NC and PC coatings. SEM observes the cracking or detachment of corrosion products on PC zinc coatings while macropits in the corrosion product layer on NC ones. EIS characteristics

change interestingly with the evolution of corrosion processes on both zinc coatings, being suitable to characterize the corrosion behavior of NC materials.

Acknowledgment The financial support provided by Natural Science Foundation of China (NSFC) in combination with Shanghai BaoSteel Company (grant No. 50471105) is greatly appreciated.

References

1. Gleiter H (1989) Prog Mater Sci 33:223
2. Kim SH, Erb U, Aust KT, Gonzalez F, Palumbo G (2004) Plat Surf Finish 91:68
3. Schneider M, Pischang K, Worch H, Fritsche G, Klimanek P (2000) Mater Sci Forum 873:343–346
4. Rofagha R, Langer R, El-Sherik AM, Erb U, Palumbo G, Aust KT (1991) Scripta Metal Mater 25:2867
5. Rofagha R, Erb U, Ostander D, Palumbo G, Aust KT (1993) Nanostruct Mater 2:1
6. Barbucci A, Farne G, Mattaezzi P, Riccieri R, Cereisola G (1999) Corros Sci 41:463
7. Lopez-Hirata VM, Arce-Estrada EM (1997) Electrochim Acta 42:61
8. Li Y, Wang FH, Liu G (2004) Corrosion 60:891
9. Wang LP, Zhang JY, Gao Y, Xue QJ, Hua LT, Xu T (2006) Scripta Mater 55:657
10. Zidoune M, Grosjean MH, Roue L, Huot J, Schulz R (2004) Corros Sci 46:3041
11. Balyanov A, Kutnyakova J, Amirkhanova NA (2004) Scripta Mater 51:225
12. Wang SG, Shen CB, Long K, Yang HY, Wang FH, Zhang ZD (2005) J Phys Chem B 109:2499
13. Wang SG, Shen CB, Long K, Zhang T, Wang FH, Zhang ZD (2006) J Phys Chem B 109:377
14. Yu JK, Han EH, Lu L, Wei XJ, Leung M (2005) J Mater Sci 40:1019
15. Ghosh SK, Dey GK, Dusane RO, Grover AK (2006) J Alloys Compd 426:235
16. Intrui RB, Szklarska-Smialowska Z (1992) Corrosion 48:398
17. Wang XY, Li DY (2002) Electrochim Acta 47:3939
18. Ye W, Li Y, Wang FH (2006) Electrochim Acta 51:4426
19. Juarez BH, Alonso C (2006) J Appl Electrochem 36:499
20. Youssef KhMS, Koch CC, Fedkiw PS (2004) J Electrochem Soc 151:C103
21. Saber Kh, Koch CC, Fedkiw PS (2003) Mater Sci Eng A 341:174
22. Gomes A, da Silva Pereira MI (2006) Electrochim Acta 51:1342
23. Li MC, Jiang LL, Zhang WQ, Qian YH, Luo SZ, Shen JN (2007) J Solid State Electrochem 11:549
24. Youssef KhMS, Koch CC, Fedkiw PS (2004) Corros Sci 46:51
25. Cullity BD (1978) Elements of X-ray diffraction, 2nd edn. Addison-Wesley, Philippines
26. Suzuki I (1985) Corros Sci 25:1029
27. Graedel TE (1989) J Electrochem Soc 136:193C
28. Chung SC, Sung SL, Hsien CC, Shih HC (2000) J Appl Electrochem 30:607
29. Yan H, Downes J, Boden PJ, Harris SJ (1996) J Electrochem Soc 143:1577
30. Manov S, Lamazouere AM, Aries L (2000) Corros Sci 42:1235
31. Deslouis C, Duprat M, Tulet-Tournillon C (1984) J Electroanal Chem 181:119
32. Levie RD (1963) Electrochim Acta 8:751
33. Park JR, Macdonald DD (1983) Corros Sci 23:295
34. Li MC, Zeng CL, Luo SZ, Shen JN, Lin HC, Cao CN (2003) Electrochim Acta 48:1735
35. da Silva PSG, Costa ANC, Mattos OR, Correia DN, de Lima-Neto P (2006) J Appl Electrochem 36:375
36. Yadav AP, Nishikata A, Tsuru T (2004) Corros Sci 46:361
37. de la Fuente D, Castano JG, Morcillo M (2007) Corros Sci 49:1420
38. Chung SC, Cheng JR, Chiou SD, Shih HC (2000) Corros Sci 42:1249
39. Park H, Szpunar JA (1998) Corros Sci 40:525
40. Yadav AP, Nishikata A, Tsuru T (2005) J Electroanal Chem 585:142
41. Barranco V, Feliu S Jr, Feliu S (2004) Corros Sci 46:2203
42. Cachet C, Wiart R (1981) J Electroanal Chem 129:103